

Selective Insulation of Carbon Nanotubes

Gabriel Dunn, Konlin Shen, Hamid Reza Barzegar, Wu Shi, Jason N. Belling, Tran N. H. Nguyen, Emil Barkovich, Kyle Chism, Michel M. Maharbiz, Michael R. DeWeese, and Alex Zettl*

We demonstrate a method for the selective encapsulation of carbon nanotubes in thin parylene films using iron as a sacrificial lift-off layer. The iron serves as an inhibitor of parylene deposition and prevents the parylene molecules from linking, thus facilitating selective area coating after lift-off.

1. Introduction

Carbon nanotubes (CNTs) have a number of remarkable properties making them suitable for application as nano-electrodes. CNTs have a high Young's modulus, allowing for stable aspect ratios many times those achievable with other materials.^[1] They are electrically conductive and can be extremely electrochemically active.^[2] Furthermore, a number of facile routes to tube functionalization have been reported.^[3–6]

Due to these properties, CNTs have found application as electrochemical probes and ultra-high resolution conductive atomic force microscopy (AFM) tips.^[7–11] Additionally, CNTs

have been employed as cellular probes, where their small cross-sectional area allow them to pierce cells with little to no effect on cell viability.^[12–14] Combined with the rich electrochemical properties of CNTs, this suggests they are ideal candidates for nanoscale bio-electrodes.^[15]

A useful CNT modification is the selective insulation of CNTs, where all but the tip of the probe is covered by an electrical insulator. Even in the case of

standard non-conductive AFM, an added layer can act as a means of improving the rigidity and durability of the device. As the buckling strength of a tube scales with R^4 —where R is the tube radius—coating materials with much smaller Young's modulus compared to the CNT can still have a significant impact.^[11] While dielectric films such as Al_2O_3 deposited by atomic layer deposition (ALD) have commonly been used to insulate CNTs for use as a transistor,^[16–17] they prove too brittle for the insulation of a cantilevered probe. During use, small displacements of the nanotube can cause the dielectric film to break and quickly begin to chip off. Polymer insulation insulating films are a promising alternative.

Parylene C, in particular, is a clear candidate for nanoprobe passivation. Parylene is a trade name for the class of poly(p-xylylene) polymers, while Parylene C specifically contains a single chlorine group, as shown in **Figure 1a**. It is flexible enough to bend with the CNT and is extremely chemically inert, a useful property for electrochemical applications. It has also been shown to be biocompatible, useful for applications as a cellular probe,^[18–19] and has demonstrated a high mechanical strength.^[20] And, the gas phase deposition method of parylene conformally coats a substrate, ensuring that the entire circumference of the tube is insulated, and has been shown to be pinhole free at thicknesses as low as 50 Å.^[21] Furthermore, parylene has shown a high affinity for coating CNTs, as shown in **Figure 1b**, likely due to π - π stacking interactions between the base layer of the polymer and the tube.^[22]

However, many of these strengths also make patterning parylene difficult. The conformal coating means that standard lift-off process that rely on anisotropic film deposition will not work. The chemical resistance of parylene also makes wet etch removal difficult. Oxygen plasma has been used to etch and pattern parylene, but doing so would often damage the underlying carbon nanotube.^[23] Miserendino et al. have demonstrated that by tuning the plasma conditions, parylene could be etched at a faster rate than the CNT, effectively exposing nanotubes. However, nanotube etching does still occur, meaning this method lacks exposure length control without sacrificing the

G. Dunn, Dr. H. R. Barzegar, Dr. W. Shi,
J. N. Belling, T. N. H. Nguyen, E. Barkovich,
K. Chism, Prof. M. R. DeWeese, Prof. A. Zettl
Department of Physics, University of California
at Berkeley, Berkeley, CA 94720, USA
E-mail: azettl@berkeley.edu


G. Dunn, Dr. H. R. Barzegar, Dr. W. Shi, Prof. A. Zettl
Materials Sciences Division, Lawrence Berkeley
National Laboratory, Berkeley, CA 94720, USA

G. Dunn, Dr. H. R. Barzegar, Dr. W. Shi, J. N. Belling,
T. N. H. Nguyen, E. Barkovich, K. Chism, Prof. A. Zettl
Kavli Energy NanoScience Institute at the University
of California, Berkeley and the Lawrence Berkeley
National Laboratory, Berkeley, CA 94720, USA

K. Shen, Prof. M. M. Maharbiz
UCB/UCSF Joint Graduate Program in
Bioengineering, University of California at Berkeley,
Berkeley, CA 94720, USA

Prof. M. M. Maharbiz
Department of Electrical Engineering and
Computer Sciences, University of California at
Berkeley, Berkeley, CA 94720, USA

Prof. M. R. DeWeese
Helen Wills Neuroscience Institute and Redwood
Center for Theoretical Neuroscience, University of
California at Berkeley, 132 Barker Hall, Berkeley, CA 94720, USA

 The ORCID identification number(s) for the author(s) of this article
can be found under <https://doi.org/10.1002/pssb.201700202>.

DOI: 10.1002/pssb.201700202

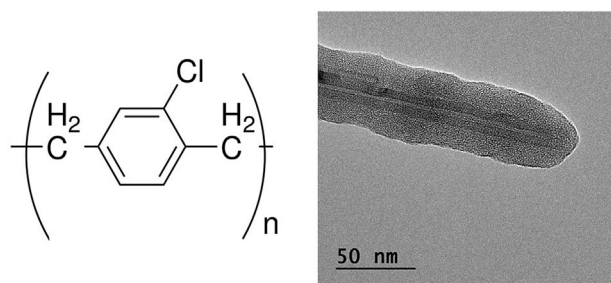


Figure 1. Parylene C for insulating carbon nanotubes. (a) Chemical structure of Parylene C. (b) TEM image of CNT coated in 25 nm of parylene C. The CNTs were uniformly coated, and no pinholes or other defects are seen in the parylene insulation.

condition of the tube and is unsuitable for the planar processing of individual CNTs.^[24] Other work has relied on either the thermal decomposition of parylene to expose the tip of a polymer coated CNT, using MEMS heaters or lasers to melt away parylene at the tip, or the physical removal of the polymer.^[10,15,25–26] Unfortunately, these methods also make tailoring the size of the exposed tip difficult and have extremely low yields, making them unsuitable for large scale application.

Here, we employ a planar process for selectively insulating a carbon nanotube probe with parylene that allows us to precisely control the length of exposed tube. It has previously been shown that parylene deposition on transition metals is inhibited by chemical deactivation and desorption of the polymer, resulting in highly non-uniform deposition.^[21,27] Here, we show that if the polymer islands are not yet large enough to form a continuous network, the transition metal can be chemically etched, lifting off the parylene as well. Hence, by utilizing a sacrificial layer of iron on areas of the tube we wish to leave exposed, we are able to lift off incomplete parylene networks, re-exposing the underlying nanotube.

2. Methods

While parylene deposition can be very uniform, it has been observed that deposition on transition metals typically results in highly non-uniform films. As described by Vaeth and Jensen,^[27] the transition metal serves to limit both the initiation and

propagation of parylene growth. Parylene molecules more readily desorb from the transition metal substrate, and when adsorbed are often deactivated and fail to form polymer chains. Over time, active parylene molecules will adsorb onto the metal, serving as nucleation sites that grow with further deposition. After sufficient deposition, the nucleation sites will grow together to create a continuous film. If we limit the amount of parylene deposited so that the nucleation sites are not able to form a continuous film, when the transition metal is removed, the disjoint parylene islands will lift-off as well, as shown in the schematic in **Figure 2**.

To first demonstrate that this method is effective in the selective removal of parylene films, parafilm is used as a shadow mask to deposit 50 nm of Fe by electron beam evaporation onto half of a Si chip. A 60 nm thick film of Parylene C is deposited using a Specialty Coating Systems Parylene Deposition System 2010 Labcoater 2. The chip is then placed in a 20% nitric acid etch at room temperature for 1 min to remove the iron and the parylene islands that had been forming. The parylene layer is then evaluated by AFM and Scanning Electron Microscopy (SEM).

This method of selective thin film parylene deposition and removal lends itself to the selective encapsulation of carbon nanotubes, in which other methods of parylene removal, such as oxygen plasma or ion milling, may damage the underlying nanotube. To verify that this method results in fully exposed nanotubes, a multi-walled CNT (Sigma Aldrich) IPA solution is dropcast onto a Transmission Electron Microscopy (TEM) grid. A glass slide is placed on top of half of the grid to serve as a shadow mask, while 50 nm of Fe is evaporated onto the grid. Parylene is then deposited onto the grid as described earlier. The grid is then floated on a 20% nitric acid solution for 20 s to remove the Fe, then transferred to two sequential water baths to remove any excess nitric acid. The grid is then imaged under TEM to verify the absence of parylene in regions which had been coated in iron and the presence of parylene in the uncoated regions.

This method can also be applied to individual nanotubes in order to leave an exposed region of controllable length, while leaving the rest of the tube encapsulated. Shown schematically in **Figure 3**, MWCNTs are suspended in ortho-dichlorobenzene to direct the placement of an array of tubes as described previously^[28] and in more detail in the Supporting Information.

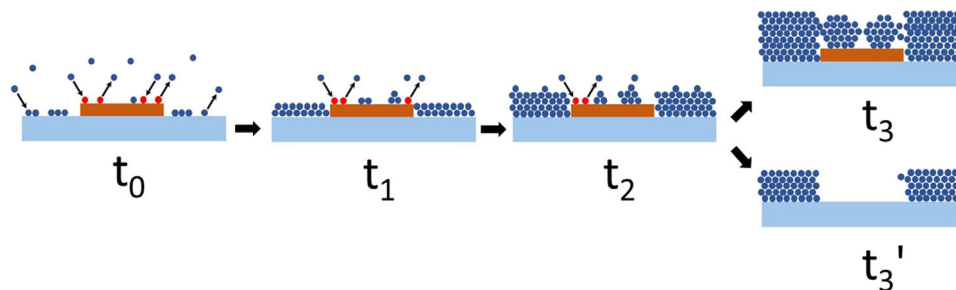


Figure 2. Schematic of selective parylene deposition on iron film. At times t_0 – t_2 , parylene deposits uniformly on substrate, but readily desorbs and is often deactivated (shown in red) on the Fe film. Nucleation sites eventually form and grow on Fe. At t_3 , the nucleation sites have grown together to create a continuous film (upper arrow). Alternatively, if the iron is removed before the nucleated areas have grown together, the incomplete parylene islands are lifted off as well (lower arrow).

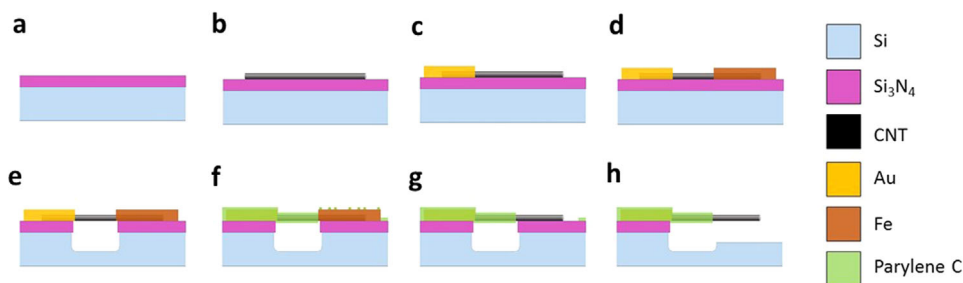


Figure 3. Schematic of selective parylene encapsulation of individual CNT process. (a) Si_3N_4 is deposited by CVD onto a silicon wafer, which is then diced. (b) CNTs are controllably placed on the substrate following the method outlined in Ref. [28] and Supporting Information. They are suspended in ODCB by sonication and drop-cast onto the chips in a spin-coater. (c) Au pads are patterned onto the base of the CNT by e-beam lithography and e-beam evaporator. (d) Iron pads are patterned onto the tip of the CNT by e-beam lithography and e-beam evaporator. (e) A XeF_2 vapor etch is used to undercut the tube to allow it to be fully coated in parylene. (f) Parylene C is deposited by CVD. (g) Fe and parylene are removed in 20% HNO_3 wet etch for 5 min. (h) A second XeF_2 etch is used to release the CNT. The resulting chip can be seen in detail in Figure S1.

Chrome/gold (2 nm/75 nm) contacts are patterned by electron beam lithography and electron beam evaporation at the base of the tube, serving as an electrical contact, an anchor point, and an etch mask. Similarly, a pad of Fe (75 nm) is patterned by electron beam lithography and electron beam evaporation at the tip of the tube. In order to encapsulate the full circumference of the nanotube, the underlying Si_3N_4 and Si are etched using a XeF_2 vapor phase etch (20×30 s cycles at 3.0 Torr), leaving the tube suspended. The etch area is defined by an electron beam patterned layer of PMMA, where the Fe and Au layers serve as an etch mask at either end of the tube. A thin film of Parylene C is then deposited. The chip is then placed in a 20% nitric acid solution for ~ 5 min. It is worth noting that while the etchant rapidly dissolves iron, the graphitic nanotube layers are etch resistant at this concentration. After the chemical etch, the chip is rinsed in DI water and IPA and dried in a critical point dryer to avoid damaging the suspended tube. Another XeF_2 vapor phase etch is used to etch the now parylene-free iron pad sites, releasing the nanotube (10×30 s cycles at 3.0 Torr). The complete fabrication process, as well as a detailed image of the resulting chip, are described in more detail in the Supporting Information.

3. Results

Figure 4 shows SEM and AFM images of a Si chip in which part was coated in Fe. The border between the Fe-free area where parylene is present, and the area which had been coated in Fe and is now parylene-free, can be clearly seen in the SEM. The conductive bare Si substrate shows up as a brighter contrast region in the SEM compared to the insulating parylene coated area. The AFM image in **Figure 4b** shows a chip with 60 nm of parylene deposited before the Fe has been removed by the HNO_3 etch. Very small – on the order of 10's of nanometers – particles can be seen on the iron-coated side, which are likely small areas of parylene nucleation. It is worth noting that the larger parylene particles at the border are likely due to patchy iron deposition as a shadow mask was used. The AFM image in **Figure 4c** was taken after the nitric acid etch. As can be seen, the parylene remains unaffected by the etch and the small parylene nucleation sites are now gone.

Our TEM study shows that this iron lift-off layer works on CNTs as well. **Figure 5a** shows the TEM grid in which half has been coated in Fe before parylene deposition. TEM images taken from both sides of the grid after the Fe-etch are shown in **Figure 5b**. CNTs on the side of the grid that had not been coated in iron are uniformly coated in a layer of parylene around 30 nm thick. In contrast, CNTs on the Fe-coated side are parylene free, as shown in **Figure 5c**. The CNTs on the parylene-free side of the chip show no significant indications of tube wall damage, confirming that the brief dilute nitric acid etch does not damage the CNT. There is also very little indication of residual Fe after the etch. This may be critical in using the CNT as an intracellular probe, as Fe has been shown to be cytotoxic.^[29]

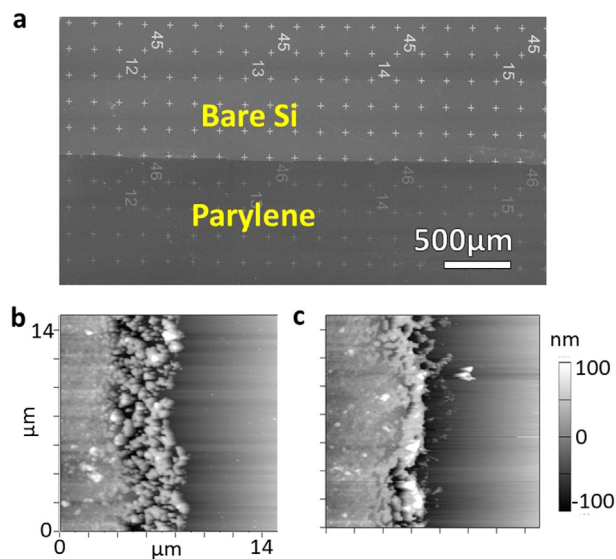


Figure 4. Parylene removal on Si chip. (a) SEM image of Si chip in which Fe has been deposited and removed on the top half, leaving bare Si, whereas parylene readily coated the bottom, Fe-free region. (b) AFM image of parylene border after 60 nm deposition, but before Fe-etch. Very small parylene nucleation sites can be seen on the right-hand side. (c) AFM image of border after Fe-etch in 20% HNO_3 for 1 min. No parylene nucleation sites can be seen on the right.

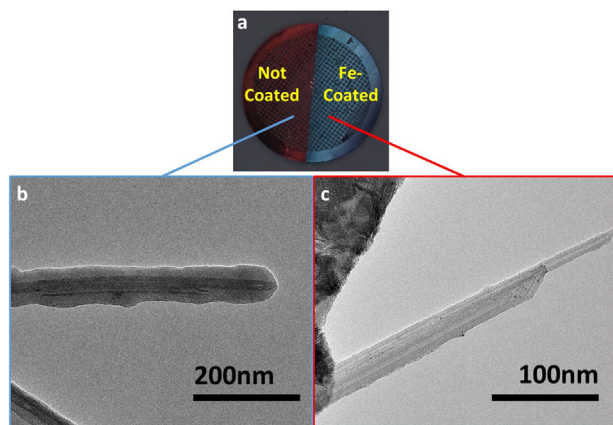


Figure 5. Parylene coverage and inhibition on CNTs. (a) Optical image of a CNT-covered TEM grid with half coated in Fe and the other half uncoated, after a 30 nm parylene deposition. (b) TEM image of parylene encapsulated nanotube on the Fe-free side of the grid. (c) TEM image of a parylene-free bundle of two CNTs which had been on the Fe-coated side of the grid, after the iron was etched by floating on HNO_3 for 20 s.

Figure 6a shows the resulting chips from the fabrication steps described above. A more detailed image can be found in Figure S2. The chip shows an array of individual nanotube sites, demonstrating that this method lends itself to large-scale, multi-unit probe fabrication. As can be seen from the SEM images in Figure 6b–e, the tip of the CNT is exposed, while the rest is uniformly coated in parylene. The length of exposed tip is 1.25 μm and can be controlled by the length of the nanotube initially coated in Fe.

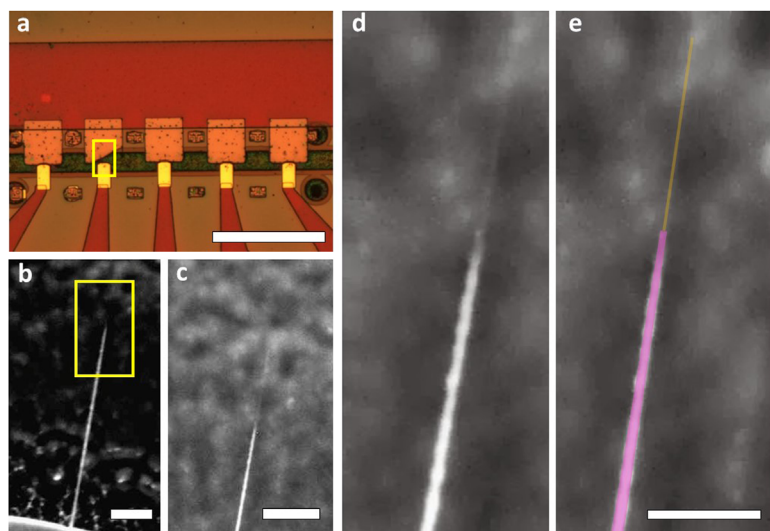


Figure 6. Selective parylene encapsulation of individual CNT. (a) Optical image of multi-unit CNT probe chip. Scale bar is 500 μm . More detailed image can be seen in Figure S2. (b)–(d) SEM images of encapsulated CNT with tip exposed. The parylene thickness in this image is 30 nm, and the CNT appears well encapsulated. Scale bars are 1 μm , 1 μm , and 500 nm respectively. (e) A false-color version of (d) to highlight the parylene-coated (purple) and exposed (yellow) regions of the CNT. The exposed length of the tube is 1.25 μm .

4. Conclusions

We have shown that by using a sacrificial layer of iron, we can inhibit parylene deposition, and selectively encapsulate a carbon nanotube with Parylene C. The parylene coats the nanotube in the exposed areas uniformly. The parylene film's flexibility allows it to flex without any evidence of cracking and is both biocompatible and chemically inert. The high yield and low likelihood of nanotube damage of this method compared to other methods of parylene removal makes it possible to use for large-scale high throughput production of insulated nanotube probes. This method of tube insulation could be extended to other nanotubes beyond carbon and could find application in nanoelectrochemistry, neural probes and conductive atomic force microscopy.

Supporting Information

Supporting Information is available from the Wiley Online Library or from the author.

Acknowledgements

This work was supported in part by the Director, Office of Science, Office of Basic Energy Sciences, Materials Sciences, and Engineering Division, of the US Department of Energy under Contract No. DE-AC02-05-CH11231, within the sp²-Bonded Materials Program (KC2207), which provided for synthesis and preliminary characterization of CNTs; and under the Nanomachines Program (KC1203), which provided for development of the parylene deposition and lift-off process; and in part by the National Science Foundation through Grant No. DMR-1206512, which provided for development of the device; and Grant No. CBET-1265085, which provided for design of the device. We also wish to thank Benji Aleman, Badr Albanna, and Aidin Fathalizadeh for their early work and ideas on the conception of this project.

Conflict of Interest

The authors declare no conflict of interest.

Keywords

carbon nanotubes, conductive atomic force microscopy, insulation, nanoelectrodes, parylene C

Received: May 3, 2017

Revised: August 3, 2017

Published online: September 25, 2017

- [1] M. M. J. Treacy, T. W. Ebbesen, J. M. Gibson, *Nature* **1996**, 381, 678.
- [2] Q. Zhao, Z. Gan, Q. Zhuang, *Electroanalysis* **2002**, 14, 1609.
- [3] S. E. Moulton, A. I. Minett, G. G. Wallace, *Carbon Nanotechnology – Recent Developments in Chemistry, Physics, Materials Science and Device Applications*. L. Dai (Ed.), Elsevier, **2006**, chapt. 11, pp. 297–312.

- [4] A. Hirsch, O. Vostrowsky, Functionalization of carbon nanotubes, in: *Functional Molecular Nanostructures*, Springer, Berlin, Heidelberg **2005**, pp. 193–237.
- [5] H. Kuzmany, A. Kukovec, F. Simon, M. Holzweber, C. Kramberger, T. Pichler, *Synth. Met.* **2004**, *141*, 113.
- [6] P. Wu, X. Chen, N. Hu, U. C. Tam, O. Blixt, A. Zettl, C. R. Bertozzi, *Angew. Chem. Int. Ed.* **2008**, *47*, 5022.
- [7] H. Dai, J. H. Hafner, A. G. Rinzler, D. T. Colbert, R. E. Smalley, *Nature* **1996**, *384*, 147.
- [8] R. M. Stevens, N. A. Frederick, B. L. Smith, D. E. Morse, G. D. Stucky, P. K. Hansma, *Nanotechnology* **2000**, *11*, 1.
- [9] N. R. Wilson, J. V. Macpherson, *Nature Nanotechnol.* **2009**, *4*, 483.
- [10] A. V. Patil, A. F. Beker, F. G. M. Wiertz, H. A. Heering, G. Coslovich, R. Vlijm, T. H. Oosterkamp, *Nanoscale* **2010**, *2*, 734.
- [11] A. Patil, J. Sippel, G. W. Martin, A. G. Rinzler, *Nano Lett.* **2004**, *2*, 303.
- [12] X. Chen, U. C. Tam, J. L. Czapinski, G. S. Lee, D. Rabuka, A. Zettl, C. R. Bertozzi, *J. Am. Chem. Soc.* **2006**, *128*, 6292.
- [13] X. Chen, A. Kis, A. Zettl, C. R. Bertozzi, *Proc. Natl. Acad. Sci. USA* **2007**, *104*, 8218.
- [14] R. Singhal, Z. Orynbayeva, R. V. K. Sundaram, J. J. Niu, S. Bhattacharyya, E. A. Vitol, M. G. Schrlau, E. S. Papazoglou, G. Friendman, Y. Gogotsi, *Nature Nanotechnol.* **2011**, *6*, 57.
- [15] T. Kawano, C. Y. Cho, L. Lin, 2nd IEEE International Conference NEMS'07, **2007**, pp. 895–898.
- [16] S. K. Kim, Y. Xuan, P. D. Ye, S. Mohammadi, J. H. Back, M. Shim, *Appl. Phys. Lett.* **2007**, *90*, 163108.
- [17] A. Javey, H. Kim, M. Brink, Q. Wang, A. Ural, J. Guo, H. Dai, *Nature Mater.* **2002**, *1*, 241.
- [18] T. Y. Chang, V. G. Yadav, S. De Leo, A. Mohedas, B. Rajalingam, C. L. Chen, A. Khademhosseini, *Langmuir* **2007**, *23*, 11718.
- [19] C. Hassler, R. P. von Metzen, P. Ruther, T. Stieglitz, *J. Biomed. Mater. Res. B, Appl. Biomater.* **2010**, *93*, 266.
- [20] V. C. Y. Shih, T. A. Harder, Y. C. Tai, IEEE Symposium on Design, Test, Integration and Packaging of MEMS/MOEMS, **2003**, pp. 394–398.
- [21] J. J. Senkevich, P. Wang, *Chem. Vap. or Deposit.* **2009**, *15*, 91.
- [22] C. L. Chen, E. Lopez, Y. J. Jung, S. Müftü, S. Selvarasah, M. R. Dokmeci, *Appl. Phys. Lett.* **2008**, *93*, 093109.
- [23] E. Meng, P. Y. Li, Y. C. Tai, *J. Micromech. Microeng.* **2008**, *18*, 045004.
- [24] S. Miserendino, J. Yoo, A. Cassell, Y. C. Tai, *Nanotechnology* **2006**, *17*, S23.
- [25] A. V. Patil, R. Vlijm, T. Oosterkamp, *NSTI-Nanotech.* **2006**, *1*, 21.
- [26] A. Inaba, Y. Takei, T. Kan, K. Matsumoto, I. Shimoyama, IEEE 16th International Conference on Solid-State Sensors, Actuators and Microsystems, **2011**, pp. 2586–2589.
- [27] K. M. Vaeth, K. F. Jensen, *Chem. Mater.* **2000**, *12*, 1305.
- [28] T. D. Yuzvinsky, A. M. Fennimore, A. Kis, A. Zettl, *Nanotechnology* **2006**, *17*, 434.
- [29] J. W. Eaton, M. Qian, *Free Radic. Biol. Med.* **2002**, *32*, 833.